ORIGINAL ARTICLE

CONTENTS

Features of structural organization of the urinary bladder under conditions of experimentally modeled hyperglycemia

Nadiya S. Tokaruk[1], Andrii O. Yurakh[2], Oksana H. Popadynets[1], Liliia V. Sobol[1], Mykhailo B. Pastukh[1], Larysa Ya. Fedoniuk[3]

[1]IVANO-FRANKIVSK NATIONAL MEDICAL UNIVERSITY, IVANO-FRANKIVSK, UKRAINE
[2]STATE INSTITUTION "ACADEMICIAN O.F. VOZIANOV INSTITUTE OF UROLOGY OF THE NATIONAL ACADEMY OF UKRAINE", KYIV, UKRAINE
[3]I. HORBACHEVSKY TERNOPIL NATIONAL MEDICAL UNIVERSITY, TERNOPIL, UKRAINE

ABSTRACT

Aim: To establish the features of morphofunctional organization of the rat urinary bladder in modeled hyperglycemia, taking into account the complex of structural-metabolic changes in the organism in the dynamics of its development.

Materials and Methods: The work was performed in compliance with the rules of humane treatment in experiments on 80 one-year-old male Wistar rats. Streptozotocin diabetes was modeled in 50 animals by single intraperitoneal administration of streptozotocin with material collection on days 14, 28, 42, 56, and 70 of the experiment. Histological, electron microscopic, biochemical, massometric methods, measurement of consumed water and daily diuresis, morphometric methods, cluster analysis, and statistical methods were applied.

Results: Urothelial cells form four clusters with histometric and ultrastructural characteristics. Chronological features of streptozotocin diabetes development were confirmed by blood glucose level, glycosylated hemoglobin content, urine glucose concentration, its pH, massometric indicators of body weight and urinary bladder weight, and volumes of consumed liquid and diuresis. Disruption of structural-functional balance between urothelial cell clusters is detected from day 14 until the end of the experiment. On days 14-28 of streptozotocin diabetes development, compensatory hypertrophy of smooth myocytes of the bladder wall with ultrastructural signs of their functional stress was detected, as well as the first signs of diabetic microangiopathy in the bladder wall. From day 56, generalization of sludge syndrome, dystrophic changes in endotheliocytes, and basement membrane edema are observed. Against the background of pronounced microangiopathy, diuresis and polydipsia decrease, desquamation of urothelial cells intensifies, and dehydration of smooth myocytes and urothelial cells occurs, which is pronounced on day 70 of the experiment.

Conclusions: In the dynamics of induced hyperglycemia development, disruption of structural-functional balance between urothelial cell clusters was detected, leading to imbalance between proliferative potentials of basal urothelial cells and integrity of the urothelial cellular barrier, as well as stages of differentiation of intermediate urothelial cells. Diabetic microangiopathy intensifies until day 70 of the experiment. Overall, during this period, diabetic cystopathy remains compensated (percentage of smooth myocyte area is 1.16 times greater than control and percentage of collagen fiber area is 1.23 times less than control).

KEYWORDS: urinary bladder, hyperglycemia, urothelium, diabetic cystopathy, microangiopathy

Wiad Lek. 2026;79(7):1556-1562. doi: 10.36740/WLek/225987 DOI

INTRODUCTION

The prevalence of diabetes mellitus has pandemic characteristics [1,2]. Almost half a billion people in the world live with diabetes mellitus, and it is predicted that their number will increase by 25% by 2030 and by 51% by 2045 [3]. Diabetes mellitus increases the risk of developing urological disorders, while urological pathology can cause decompensation of diabetes course [4]. In the lower urinary tract, complex interaction of neuronal, myogenic, and urothelial dysfunction causes the development of functional disorders, among which disorders of accumulation and emptying of the urinary bladder occupy a leading place [5]. Diabetic cystopathy is one of the specific complications of diabetes mellitus and significantly reduces the quality of life of patients from both social and economic points of view, and complicates the course of diabetes mellitus itself, which indicates the social significance of further research on this scientific topic [6,7].

Works in which the results of morphological and morphometric studies of structural components of the urinary bladder are correlated against the background of streptozotocin diabetes development with biochemical indicators of urine, which is aggressive to the urothelium, are few [8,9]. Diabetic cystopathy is associated primarily with dysfunction of the detrusor muscle of the urinary bladder, which leads to changes in its contractile ability, but research results are

ambiguous [10,11]. Changes in the urinary excretory capacity of the urinary bladder occur with structural reorganization of its muscular coat, but information on this issue is contradictory [12-14]. The connection between urodynamic disorders in diabetes mellitus and microvascular complications has been clinically proven [15,16]. However, these results are not confirmed by morphological changes in vessels and their metric characteristics. Therefore, the study of reorganization of urothelial cells, smooth myocytes, collagen fibers, and blood vessels of the urinary bladder wall during the development of diabetic cystopathy requires comprehensive research using morphological, morphometric, biochemical methods and multidimensional statistics methods.

AIM

To investigate light-optical, morphometric, and ultrastructural reorganization of urothelial cells and their cluster structures, smooth myocytes, and collagen fibers at stages of experimental streptozotocin diabetes course; to trace chronological features of microvessel changes during the development of diabetic microangiopathy in the urinary bladder wall.

MATERIALS AND METHODS

The study was conducted on 80 one-year-old male Wistar rats weighing 214-256 g. The animals were divided into three groups: intact/normal (10 animals); experimental (50 rats in which streptozotocin diabetes was modeled by single intraperitoneal administration of Sigma (USA) streptozotocin in 0.1 M citrate buffer (6 mg/100 g animal body weight)); control (20 animals - only citrate buffer was administered). Material collection for morphological and biochemical studies, determination of rat body weight and their urinary bladder weights were performed in the morning on an empty stomach on days 14, 28, 42, 56, and 70 of the experiment. Euthanasia was performed under thiopental anesthesia. The work performed does not contradict the basic bioethical norms of the Helsinki Declaration adopted by the General Assembly of the World Medical Association, the Council of Europe Convention on Human Rights and Biomedicine, relevant provisions of WHO, the International Council of Medical Scientific Societies, the International Code of Medical Ethics, and Directive 2010/63/EU of the European Parliament and Council of Europe on the protection of animals used for scientific purposes. Histological sections were stained with hematoxylin and eosin and by Masson's trichrome method. Semi-thin sections were stained with 1% methylene blue solution. Electron micrographs were digitized on an Epson Perfection V550 Photo scanner at 1200 dpi resolution. Blood glucose level (mmol/L) was studied by glucose oxidase method. Glycosylated hemoglobin (HbA1C) content in blood (%) was determined using the "ACCENT-200 HbA1c DIRECT" kit (PZ Cormay S.A., Poland). Urine pH was measured with a portable "Checker 1" pH meter (Hanna Instruments, Italy).

RESULTS

Using Ward's cluster analysis method (Euclidean metric), it was determined that the cluster structure of transitional epithelium cells of the urinary bladder consisted of 4 clusters, with cell percentages equal to 10.96, 39.47, 34.21, and 15.35%, respectively. It was established that normally, the percentages of cells falling into clusters 1 and 4 and clusters 2 and 3 did not differ significantly from each other ($p>0.05$). Cluster 1 is represented by basal urothelial cells that were poorly differentiated, as indicated by their high nuclear-cytoplasmic ratio (NCR) (0.81±0.30). They are the smallest in area (42.2±5.09) μm^2 and nuclear area (18.3±4.79) μm^2. Their features include attachment to the basement membrane of the urothelium and paucity of organelles. We determined that cluster 4 is formed by umbrella cells that had the lowest NCR (0.49±0.18) and were highly differentiated. These are the largest cells by area (115.6±11.18) μm^2 and their nuclear area (36.7±7.84) μm^2. They had plaque and hinge-like regions, junctional complexes, many urothelial vesicles and primary and secondary lysosomes, and a well-developed Golgi complex. We found that clusters 2 and 3 are urothelial cells of the intermediate layer of the transitional epithelium of the urinary bladder. Cluster 3 cells characterized the final stage of intermediate urothelial cell differentiation, while cluster 2 represented the initial stage, which was argued by the following: cluster 3 urothelial cells were located under umbrella cells, while cluster 2 cells were closer to the basement membrane of the urothelium; the NCR of cluster 3 cells was (0.62±0.20), while cluster 2 was (0.79±0.28), indicating a higher degree of differentiation of cluster 3 cells; in terms of cell size (85.4±7.48) μm^2 and their nuclei (31.7±6.58) μm^2, cluster 3 urothelial cells were more mature cells than cluster 2, which were smaller - (62.5±6.21) μm^2 and (26.8±5.05) μm^2, respectively; according to ultrastructural cell structure, cluster 3 cells differed little from umbrella cells, i.e., belonged to highly differentiated cells, while cluster 2 belonged to moderately differentiated cells.

In the experiment, we established that blood glucose level increased until day 42 (by 4.75 times, $p<0.01$),

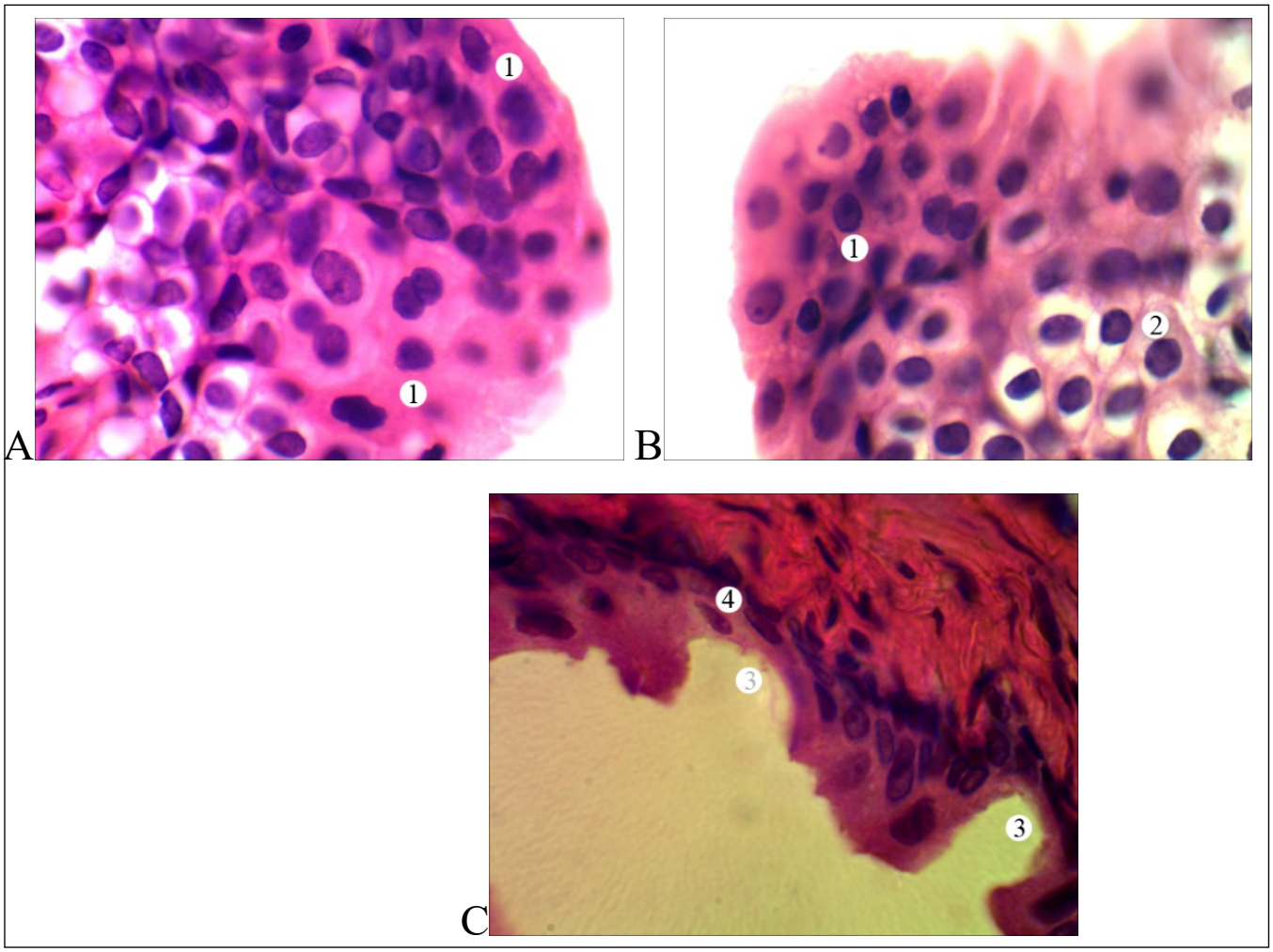

Fig. 1. Urinary bladder wall at different stages of experimentally induce hyperglycemia. A - Day 14 of the experiment: (1) umbrella urothelial cells. B - Day 28 of the experiment: (1) umbrella urothelial cells; (2) vacuolated epithelial cells of the intermediate and basal layers. C - Day 56 of the experiment: (3) loci of desquamation; (4) basal layer of the transitional epithelium. Staining: hematoxylin and eosin. Magnification: (A, B) ×400; (C) ×200.

reaching a level of (24.98±2.16) mmol/L, and did not change until the end of the experiment ($p>0.05$). Urine glucose content increased 21.38-fold ($p<0.01$) by day 42 of the experiment and did not change thereafter ($p>0.05$). HbA1C content in blood increased significantly already on day 14 of the experiment (by 3.48 times, $p<0.01$), and by day 70 became 5.34 times greater than control ($p<0.01$). The most acidic urine reaction was determined on day 56 of the experiment. Body weight of diabetic rats gradually decreased and by day 70 of the experiment became 1.46 times less than control ($p<0.01$). The amount of water consumed by diabetic rats and daily diuresis increased by day 28 of the experiment by 7.61 and 18.54 times respectively ($p<0.01$), and by the end of the experiment decreased somewhat but remained greater than control, by 5.84-4.90 and 13.64-11.10 times respectively ($p<0.01$).

In streptozotocin diabetes, structural-functional balance between cells was disrupted due to an increase in the percentage of cluster 1 cells ($p<0.001$) and a decrease in clusters 3 and 4 ($p<0.01$) with no changes in the proportion of cluster 2 cells ($p>0.05$), which indicated disorganization (imbalance) of systemic mechanisms of urothelial functioning, which occurred from the first terms of the experiment. It was established that the cause of these changes is desquamation of urothelial cells, which led to disruption of morphological stratification of the urothelium, which became one- or two-layered.

We established that by day 28 of the experiment, hypertrophy of smooth myocytes developed, which was morphometrically confirmed by an increase in their area percentage by 1.31 times ($p<0.001$), and ultrastructurally by signs of functional stress (light myocytes with clearly expressed myofilaments that had large nuclei with numerous protrusions and invaginations of the nuclear envelope; in the cytoplasm - a large number of free ribosomes and glycogen inclusions located near the nuclear poles; increased size and content of mitochondria detected near nuclei or in sarcoplasm).

Simultaneously, the percentage of collagen fiber area decreased by 1.92 times ($p<0.001$), which is a compensatory reaction that provided the possibility of bladder wall stretching.

We established that diabetic microangiopathy of the urinary bladder was determined by sludge, the degree and prevalence of which corresponded to HbA1C content. By day 28 of the experiment, arteriole dilation was revealed, on day 42 - spasm, and from day 56 - their secondary expansion. Dystrophic changes in capillary endotheliocytes were determined from day 28 of the experiment, and on day 42 became significant (their cytoplasm thickened, heterochromatin shifted marginally, organelle content decreased, microvilli appeared, cytoplasm thickening and microclasmatosis occurred). From day 56, dystrophic changes in endotheliocytes dynamically increased, which caused plasma permeation of perivascular connective tissue. The thickness of capillary basement membrane of the suburothelial hemomicrocirculatory bed gradually increased and on day 70 thickened by 3.22 times, and from day 56 the basement membrane became lamellar.

Results of comprehensive assessment of urinary bladder reorganization in streptozotocin diabetes showed that on days 14-28 of the experiment, primary increasing hyperglycemia triggered a cascade of changes that caused: minor glucosuria; expansion of arteriole lumen; hemoglobin glycosylation (HbA1C). This caused sludge formation in venules; increasing dystrophic changes in endotheliocytes; disruption of basement membrane structure. Large volume of urine led to significant polydipsia, desquamation of umbrella cells and reorganization of cluster structures of the urothelium, compensatory hypertrophy of smooth myocytes, and an increase in their area percentage. Vacuolar dystrophy developed and urothelial cell sizes increased (Fig. 1A, 1B). Arteriole expansion, polydipsia, and sludge in venules caused the development of interstitial edema.

On days 42-70 of the experiment, persistent high hyperglycemia caused: pronounced glucosuria; narrowing of arteriole lumen; sludge formation in capillaries, and from day 56 - generalization of sludge syndrome; significant dystrophic changes in capillary endotheliocytes and lamellation and thickening of their basement membranes. Diuresis and polydipsia decreased. Plasma permeation increased. Against the background of pronounced microangiopathy, myocyte dehydration occurred with a decrease in their area and an increase in the content of dark involutive types and an increase in collagen fiber area; desquamation of cells of all urothelial layers developed, and in combination with glucosuria - their dehydration and size reduction (Fig. 1C).

DISCUSSION

Taking into account our own results and literature data, it can be stated that normally, the levels of cell proportions in clusters 1 and 4 indicate structural-functional balance between proliferation of basal cells and integrity of the urothelial cellular barrier, and the levels of cell proportions in clusters 2 and 3 indicate balance between initial and final stages of differentiation of intermediate urothelial cells [17]. Basal urothelial cells are cambial committed cells that differentiate into cells of other layers of transitional epithelium [18]. Cluster 4 urothelial cells form the urothelial cellular barrier [19,20]. A number of authors identify an additional type of urothelial cells located under umbrella cells and capable of quickly replacing them in case of damage [21,22] - these were cluster 3 cells.

In the experiment, we established that blood glucose level increased until day 42 (by 4.75 times, $p<0.01$), reaching a level of (24.98±2.16) mmol/L, and did not change until the end of the experiment ($p>0.05$). Authors who used Wistar rats indicate the same dynamics of hyperglycemia development [23]. In contrast, in experiments involving Sprague-Dawley rats, blood glucose levels of 21-28 mmol/L are observed already on days 3-14 from induction of streptozotocin diabetes [24].

The decrease in body weight of experimental animals is associated with protein metabolism disorders. We used one-year-old rats, in which the insignificant natural increase in body weight could not affect the experiment results, based on the fact that in recent years there have been data proving the dependence of body weight decrease in animals with streptozotocin diabetes on sex, rat line, and especially on age[25,26]. It was found that the urinary bladder weight of diabetic rats increased by day 70 by 1.57 times ($p<0.01$).

On days 14-28 of the experiment, the area of urothelial cells ($p<0.001$) and their nuclei ($p<0.01$) of all clusters increased due to the development of vacuolar dystrophy triggered by hyperglycemia, which led to an 18.54-fold increase (day 28) in daily urine volume. The development of vacuolar dystrophy can be explained by the fact that as a result of a multiple increase in diuresis rate, urine against the background of minor glucosuria became of low specific gravity. The movement of such (hypotonic) urine into the depth of the urothelium was facilitated by desquamation of its cells and wedge-shaped ruptures that sometimes reached the basement membrane of the urothelium. Water transport to urothelial cells occurred passively - as a result of diffusion along a concentration gradient. On days 42-70 of the experiment, persistent significant glucosuria against the background of decreased polyuria increased urine specific gravity, which led to

dehydration of urothelial cells, decrease in their area and nuclei ($p<0.01$), and ultrastructural reorganization (ruptures of junctional complexes; osmiophilic cytoplasm matrix; fusion of vacuoles into balloons that compressed the nucleus and organelles; short cisterns of granular endoplasmic reticulum and Golgi complex; small mitochondria with crest destruction and dark matrix; secondary lysosome disintegration; decreased content of urothelial vesicles).

From day 42 of the experiment, the percentage of collagen fiber area increased and smooth myocyte area decreased, but even on day 70, the myocyte area proportion remained greater than control (by 1.16 times, $p<0.001$), indicating their hypertrophy, while collagen fibers were less (by 1.23 times, $p<0.001$), and there was no basis to speak of diffuse fibrosis of the bladder wall. This indicates that diabetic cystopathy remained compensated during our experiment. From day 56, the content of dark myocytes of involutive type with paucity of organelles, subsarcolemmal vesicles, and myofilaments increased. Myocytes with sarcolemma sequestration and individual areas of interstitial substance fibrosis were detected. The obtained results are consonant with data from other researchers [27].

It is known that primary hyperglycemia causes release of vasodilators, and high hyperglycemia causes vasoconstrictors [28,29]. Secondary expansion of microvessels is due to disruption of their sympathetic innervation.

Such dynamics of morpho-functional changes was traced when studying the effect of experimental streptozotocin diabetes on seromucous cells of the submandibular salivary gland. The authors state that the reaction of glandulocytes of seromucous acini to hyperglycemia development is typical and non-specific. Alterative changes have a pronounced dystrophic character in early stages and increase until day 42 of the experiment. On day 70, histological adaptation of seromucous cells was observed, which is confirmed by the development of atrophic changes, decrease in cell area, and normalization of the relative area of their granules [30].

CONCLUSIONS

In the dynamics of experimental streptozotocin diabetic cystopathy development, two periods can be distinguished. The first lasts during days 14-28 and manifests as increasing hyperglycemia and glucosuria, pronounced polyuria and polydipsia, reorganization of cluster structures of urothelial cellular composition, desquamation of umbrella cells and wedge-shaped ruptures of the urothelium, increase in area and vacuolar dystrophy of urothelial cells, compensatory hypertrophy of smooth myocytes of the bladder wall, and development of initial signs of diabetic microangiopathy. The second period covers days 42-70 and is characterized by high stable hyperglycemia and glucosuria, decrease compared to day 28 in polyuria and polydipsia, dehydration of urothelial cells (with corresponding qualitative and morphometric changes) and smooth myocytes (with decrease in their area proportion and prevalence of dark involutive types), occurring against the background of pronounced diabetic microangiopathy.

REFERENCES

1. Szwarcbard N, Xiang A, Gasevic D, Jones A, Earnest A, Andrikopoulos S, et al. The association of weight status with glycemic control, diabetes related complications and anti-hyperglycemic medication use in patients with type 2 diabetes mellitus: The results of the Australian National Diabetes Audit (ANDA) 2015–2022. Diabetes Res Clin Pract. 2025;226:112333. doi:10.1016/j.diabres.2025.112333 DOI
2. Tanasescu D, Sabau D, Moisin A, Gherman C, Fleaca R, Bacila C, et al. Risk assessment of amputation in patients with diabetic foot. Exp Ther Med. 2023;25(1):12. doi:10.3892/etm.2022.11711 DOI
3. Saeedi P, Petersohn I, Salpea P, Malanda B, Karuranga S, Unwin N, et al. Global and regional diabetes prevalence estimates for 2019 and projections for 2030 and 2045: Results from the International Diabetes Federation Diabetes Atlas, 9th edition. Diabetes Res Clin Pract. 2019;157:107843. doi:10.1016/j.diabres.2019.107843 DOI
4. Ryšánková M. Diabetes mellitus urological complication. Vnitr Lek. 2023;69(E-2):26–30. doi:10.36290/vnl.2023.026 DOI
5. Rutkowski M. Functional disorders of the lower urinary tract in diabetes mellitus. Urologie. 2025;64(2):128–135. doi:10.1007/s00120-024-02506-0 DOI
6. Du H, Xu F, Liu J, Zhang J, Qin Y, Xu Y, et al. Long-term aspirin administration suppresses inflammation in diabetic cystopathy. Aging (Albany NY). 2023;15(17):9128–9143. doi:10.18632/aging.205021 DOI
7. Hindi EA, Williams CJ, Zeef LAH, Lopes FM, Newman K, Davey MMM, et al. Experimental long-term diabetes mellitus alters the transcriptome and biomechanical properties of the rat urinary bladder. Sci Rep. 2021;11(1):15529. doi:10.1038/s41598-021-94532-7 DOI
8. Wróbel A, Serefko A, Bańczerowska-Górska M, Szopa A, Dudka J, Poleszak E. Intravesical administration of blebbistatin prevents cyclophosphamide-induced toxicity of the urinary bladder in female Wistar rats. Neurourol Urodyn. 2019;38(4):1044–1052. doi:10.1002/nau.23973 DOI

9. Giaquinto D, Palladino A, Cummaro A, De Felice E, Esposito V, Moretta R, et al. Well-Preserved Urinary Bladder Anatomy in Rats After Minimally Invasive Surgery. Biomedicines. 2025;13(2):285. doi:10.3390/biomedicines13020285 DOI
10. Majima T, Matsukawa Y, Funahashi Y, Takai S, Kato M, Yamamoto T, Gotoh M. Urodynamic analysis of the impact of diabetes mellitus on bladder function. Int J Urol. 2019;26(6):618–622. doi:10.1111/iju.13935 DOI
11. Klee NS, Moreland RS, Kendig DM. Detrusor contractility to parasympathetic mediators is differentially altered in the compensated and decompensated states of diabetic bladder dysfunction. Am J Physiol Renal Physiol. 2019;317(2):F388–F398. doi:10.1152/ajprenal.00178.2019 DOI
12. Jhang JF, Jiang YH, Hsu YH, Ho HC, Kuo HC. Pathogenesis evidence from human and animal models of detrusor underactivity. Tzu Chi Med J. 2022;34(3):287–296. doi:10.4103/tcmj.tcmj_284_20 DOI
13. Shimizu S. Association of detrusor underactivity with aging and metabolic syndrome: suggestions from animal models. J Smooth Muscle Res. 2024;60:23–30. doi:10.1540/jsmr.60.23 DOI
14. Sekido N, Otsuki T, Kida J, Mashimo H, Wakamatsu D, Okada H, et al. EP2 and EP3 receptors as therapeutic targets for underactive bladder/detrusor underactivity due to diabetic cystopathy in a type 1 diabetic rat model. Low Urin Tract Symptoms. 2020;12(3):285–291. doi:10.1111/luts.12317 DOI
15. Kabuto T, Inamura S, Kobayashi H, Zha X, Nagase K, Taga M, et al. PDE5 inhibitor potentially improves polyuria and bladder storage and voiding dysfunctions in type 2 diabetic rats. PLoS One. 2024;19(9):e0301883. doi:10.1371/journal.pone.0301883 DOI
16. Kwon MH, Choi MJ, Liu FY, Fridayana FR, Niloofar L, Yin GN, et al. Functional and immunofluorescence evaluations of vascular and neural integrities in urinary bladder of streptozotocin-induced diabetic mice. Int Neurourol J. 2022;26(3):201–209. doi:10.5213/inj.2244152.076 DOI
17. Paige JT, Lightell DJ Jr, Douglas HF, Klingenberg NC, Pham T, Woods TC. Incubation with porcine urinary bladder matrix yields a late-stage wound transcriptome in endothelial cells and keratinocytes isolated from both diabetic and non-diabetic subjects. Exp Dermatol. 2023;32(9):1430–1438. doi:10.1111/exd.14845 DOI
18. Gulinac M, Velikova T, Dikov D. Multinucleated giant cells of bladder mucosa are modified telocytes: diagnostic and immunohistochemistry algorithm and relation to PD-L1 expression score. World J Clin Cases. 2023;11(26):6091–6104. doi:10.12998/wjcc.v11.i26.6091 DOI
19. Wu Z, Li Y, Liu Q, Liu Y, Chen L, Zhao H, et al. Pyroptosis engagement and bladder urothelial cell-derived exosomes recruit mast cells and induce barrier dysfunction of bladder urothelium after uropathogenic E. coli infection. Am J Physiol Cell Physiol. 2019;317(3):C544–C555. doi:10.1152/ajpcell.00102.2019 DOI
20. Jhang JF, Lin TY, Ho HC, Jiang YH, Hsu YH, Birder LA, et al. Deficits of urothelial cell proliferation, cytoskeleton, and barrier function protein expressions in patients with recurrent and persistent urinary tract infections. Low Urin Tract Symptoms. 2021;13(2):203–209. doi:10.1111/luts.12351 DOI
21. Zupančič D, Romih R. Immunohistochemistry as a paramount tool in research of normal urothelium, bladder cancer and bladder pain syndrome. Eur J Histochem. 2021;65(2). doi:10.4081/ejh.2021.3242 DOI
22. Chen J, Yu M, Wang L, Xie H, Lv Y, Huang Y, et al. KRT5(high) TP63-expressing urothelial basal cells act as a driver to bladder urothelium regeneration in rabbit. Stem Cell Res Ther. 2025;16(1):296. doi:10.1186/s13287-025-04417-z DOI
23. Saleem A, Akhtar MF, Latif A, Abdel-Daim MM, Baig MMFA, Saleem M, et al. Chemical characterisation and appraisal of antidiabetic potential of Terminalia citrina extract in streptozotocin induced hyperglycaemia in Wistar rats. Arch Physiol Biochem. 2024;130(1):56–69. doi:10.1080/13813455.2021.1963783 DOI
24. Moin H, Shafi R, Ishtiaq A, Liaquat A, Majeed S, Zaidi NN. Effectiveness of analog of Humanin in ameliorating streptozotocin-induced diabetic nephropathy in Sprague Dawley rats. Peptides. 2023;165:171014. doi:10.1016/j.peptides.2023.171014 DOI
25. Alfheeaid H, Alhowail A, Ahmed F, Zaki A, Alkhaldy A. Influence of various intermittent fasting regimens on body weight and glycemic control in streptozotocin-induced diabetic rats. Eur Rev Med Pharmacol Sci. 2023;27(23):11433–11444. doi:10.26355/eurrev_202312_34582 DOI
26. Dolo PR, Huang K, Widjaja J, Li C, Zhu X, Yao L, et al. Distal gastric mucosa ablation induces significant weight loss and improved glycemic control in type 2 diabetes Sprague-Dawley rat model. Surg Endosc. 2020;34(10):4336–4346. doi:10.1007/s00464-019-07200-3 DOI
27. Jhang JF, Hsu YH, Ho HC, Jiang YH, Lee CL, Yu WR, et al. Possible association between bladder wall morphological changes on computed tomography and bladder-centered interstitial cystitis/bladder pain syndrome. Biomedicines. 2021;9(10):1306. doi:10.3390/biomedicines9101306 DOI
28. Fei L, Xu M, Wang H, Zhong C, Jiang S, Lichtenberger FB, et al. Piezo1 mediates vasodilation induced by acute hyperglycemia in mouse renal arteries and microvessels. Hypertension. 2023;80(8):1598–1610. doi:10.1161/HYPERTENSIONAHA.122.20767 DOI
29. Hong J, Martín-Aragón Baudel M, Niloy SI, Taylor J, Mohabbat Y, Moustafa Y, et al. Arterial myocyte Pannexin 1 channel controls vascular reactivity in diabetic hyperglycemia. Circ Res. 2025;137(5):646–663. doi:10.1161/CIRCRESAHA.125.326260 DOI
30. Tokaruk NS, Popadynets OH, Bedei VI, Hryshchuk MI, Kotyk TL. Morphology of the submandibular gland's acini of rats in diabetes mellitus. Pathologia. 2020;17(3):384–389. https://pat.zsmu.edu.ua/article/view/221869/223158

This work was conducted within the research program of the Department of Human Anatomy at Ivano-Frankivsk National Medical University, as part of the project "Possibilities of Radiological and Morphological Methods for Diagnosing Diseases Caused by Endothelial Dysfunction of Multifactorial Origin" (0124U004858).

CONFLICT OF INTEREST
The Authors declare no conflict of interest

CORRESPONDING AUTHOR
Larysa Ya. Fedoniuk
Medical Biology Department
I. Horbachevsky Ternopil National Medical University
9 Valova St., Ternopil, Ukraine
e-mail: fedonyuk22larisa@gmail.com

ORCID AND CONTRIBUTIONSHIP
Tokaruk Nadiya: 0000-0003-1404-7857 A C E F
Yurakh Andrii: 0000-0003-1128-0629 D F
Popadynets Oksana: 0000-0002-2093-5984 A D E
Sobol Liliia: 0000-0002-9750-3493 C D
Pastukh Mykhailo: 0000-0002-7896-2088 A B
Larysa Fedoniuk: 0000-0003-4910-6888 B C F

A – Work concept and design, B – Data collection and analysis, C – Responsibility for statistical analysis, D – Writing the article, E – Critical review, F – Final approval of the article

RECEIVED: 18.03.2026
ACCEPTED: 29.06.2026